Low-energy laser-assisted electron-helium collisions

Sydney Geltman
JILA, University of Colorado, Boulder, Colorado 80309
(Received 16 July 1996)

Laser-assisted electron-helium scattering is studied by perturbation theory for electron energies $\leqslant 2.6$ eV and CO_2 laser intensities $\leqslant 1\times10^6$ W/cm^2. A model potential is adopted that gives a good description of the field-free elastic scattering. Results are presented for one- and two-photon processes. It is found that absorption cross sections are larger than those for emission. The dependences on electron energy at zero energy for absorption and at the $n\omega$ thresholds for emission are analyzed. The elastic scattering within the laser pulse is discussed and related to a general sum rule involving the n-photon process probabilities.
[S1050-2947(97)03105-3]

PACS number(s): 34.80.Qb, 03.65.Nk

I. INTRODUCTION

Laser-assisted collisions between electrons and rare-gas atoms have been studied in the laboratory for about 20 years. They are carried out with a CO_2 laser with pulses of about 3-μs duration and peak intensities of the order of 10^8 W/cm^2. The electron energies are the order of 10 eV in the elastic scattering range. The earlier measurements by Weingartshofer *et al.* [1–3] concentrated on large-angle scattering, where maximum probability for photon transfer may be expected, as in the case of bremsstrahlung by deflected charged particles. These measurements were in qualitative agreement with the Kroll-Watson [4] formula for low-frequency laser-assisted collisions. However, a more stringent test of this formula was provided in the recent measurements of Wallbank and Holmes [5–7] at small scattering angles ($\sim 10°$) and several laser polarization directions. The results of these measurements indicated very large discrepancies with Kroll-Watson theory, ranging from factors of $\sim 10^2$ for one-photon transfer to $\sim 10^{20}$ for five-photon transfer. In addition, they found cross sections of comparable magnitude for the two laser linear polarizations (i) parallel to $\mathbf{k}_i$ (incident electron vector) and (ii) perpendicular to $\mathbf{k}_i - \mathbf{k}_f$ (momentum transfer vector), in contrast to Kroll-Watson theory, which gives zero cross section for the latter polarization. A theoretical study by the present author [8] compared Kroll-Watson theory with perturbation theory at a low enough intensity (10^6 W/cm^2) for perturbation theory to be valid and also found large discrepancies, in support of the above experimental findings. While 10^6 W/cm^2 is about a factor of 50 below the experimental intensity, there was good qualitative agreement between the perturbation theory results and experiment in regard to the relative variations of cross section with scattering angle and incident electron energy for one- and two-photon processes.

The present work is an extension of this perturbation theory study, motivated in part by further measurements [9] in helium at very low electron energies. We adopt a model potential for electron-helium scattering that gives excellent agreement with very precise measurements of the field-free elastic scattering at all angles [10]. Thus, in the perturbative regime of intensities we may expect our results to be quite accurate. The large differences between perturbative and Kroll-Watson theory found in [8] are expected to also be present at these lower energies. The only region where the Kroll-Watson formula may be expected to be generally valid is at high enough electron energies where the first Born approximation is valid for field-free scattering. It should also be remembered that the first-Born form of this formula was given by Bunkin and Fedorov [11] eight years before the Kroll-Watson paper.

II. PERTURBATIVE EXPANSION

We follow closely the form of perturbation theory described in [8]. The integral form of the full time-dependent Schrödinger equation is

$$\psi(\mathbf{r},t)=\psi^{(0)}(\mathbf{r},t)-i\int_0^t dt'\int d\mathbf{r}'\,G(\mathbf{r}t;\mathbf{r}'t') \times H'(\mathbf{r}',t')\psi(\mathbf{r}',t'). \tag{1}$$

This describes the evolution of a field-free scattering state $\psi^{(0)}(\mathbf{r},t)=u^{(+)}_{\mathbf{k}_i}(r)e^{-iE_it}$ when subject to a laser pulse starting at $t=0$ with an interaction Hamiltonian H', and the full Green's function

$$G(\mathbf{r}t;\mathbf{r}'t')=\sum_{\mathbf{k}} u^{(+)}_{\mathbf{k}}(\mathbf{r})u^{(+)*}_{\mathbf{k}}(\mathbf{r}')e^{-iE_k(t-t')}. \tag{2}$$

The basis set $u^{(+)}_{\mathbf{k}}(\mathbf{r})$ includes the complete set of bound and scattering states that exist for the static electron-atom potential $V(r)$. The neglect of the multi-electron structure of the target atom and of exchange effects is expected to be a good approximation for low-energy electron–rare-gas atom scattering, where the polarization potential is expected to dominate. Adopting the ''acceleration'' form of the dipole interaction $H'=(1/\omega^2)\mathbf{E}\cdot\boldsymbol{\nabla}V$, taking a rectangular laser pulse $\mathbf{E}=\mathbf{E}_0\sin\omega t$, and carrying out two iterations of Eq. (1) gives the second-order perturbative wave function

$$\psi^{(2)}(\mathbf{r},t)=u_{\mathbf{k}_i}^{(+)}(\mathbf{r})e^{-iE_it}-\sum_{\mathbf{k}}\ u_{\mathbf{k}}^{(+)}(\mathbf{r})e^{-iE_kt}$$
$$\times\left\{\left(\frac{E_0}{2\omega^2}\right)M_{\mathbf{k}\mathbf{k}_i}^{(++)}\int_0^t dt'[e^{i(\omega_{kk_i}+\omega)t'}\right.$$
$$-e^{i(\omega_{kk_i}-\omega)t'}]+i\left(\frac{E_0}{2\omega^2}\right)^2\sum_{\mathbf{k}'}\ M_{\mathbf{k}\mathbf{k}'}^{(++)}M_{\mathbf{k}'\mathbf{k}_i}^{(++)}$$
$$\times\int_0^t dt'\left[\frac{1}{(\omega_{k'k_i}+\omega)}\ (e^{i(\omega_{kk_i}+2\omega)t'}-e^{i\omega_{kk_i}t'})\right.$$
$$\left.\left.-\frac{1}{(\omega_{k'k_i}-\omega)}\ (e^{i\omega_{kk_i}t'}-e^{i(\omega_{kk_i}-2\omega)t'})\right]\right\}. \quad (3)$$

This is a more complete form than that given in Eq. (8) of [8] in that it also retains the terms that contribute to the zero-photon amplitude, i.e., the second-order interference produced by the laser with the field-free elastic amplitude. Here $\omega_{kk'}=\frac{1}{2}(k^2-k'^2)$ and $M_{\mathbf{k}'\mathbf{k}}^{(++)}=\int d\mathbf{r}\ u_{\mathbf{k}'}^{(+)*}(\hat{\boldsymbol{\varepsilon}}\cdot\boldsymbol{\nabla}V)u_{\mathbf{k}}^{(+)}$, with $\hat{\boldsymbol{\varepsilon}}$ being the field polarization direction. The zero-, one-, and two-photon terms are clearly identifiable in Eq. (3). To obtain one- or two-photon transition probabilities, one projects onto $\psi^{(2)}$ with $u_{\mathbf{k}_f}^{(+)}(\mathbf{r})$, which leads to the effective transition rates and cross sections

$$\frac{d\sigma^{(1)}}{d\Omega}=\frac{1}{(2\pi)^2}\frac{k_f^2}{k_i}\left(\frac{E_0}{2\omega^2}\right)^2|M_{\mathbf{k}_f\mathbf{k}_i}^{(++)}|^2,$$

$$\frac{d\sigma^{(2)}}{d\Omega}=\frac{1}{(2\pi)^2}\frac{k_f^2}{k_i}\left(\frac{E_0}{2\omega^2}\right)^4\left|\sum_k\ \frac{M_{\mathbf{k}_f\mathbf{k}}^{(++)}M_{\mathbf{k}\mathbf{k}_i}^{(++)}}{(\omega_{kk_i}\pm\omega)}\right|^2. \quad (4)$$

In the intermediate-state denominator the $+,-$ signs go with two-photon emission and absorption, respectively. In [8] we also studied the use of the final continuum states $u_{\mathbf{k}}^{(-)}$ (with the ingoing-wave modification) and found that that form gave much poorer agreement with experiment.

III. ELECTRON-HELIUM EFFECTIVE POTENTIAL

In [8] we adopted a typical atomic potential of the form

$$V(r)=-e^{-2Zr}\left(Z+\frac{1}{r}\right)-\frac{\alpha_p}{2}\ (1-e^{-r})^6/r^4, \quad (5)$$

and for simplicity took the hydrogenic values of $Z=1$ and $\alpha_p=4.5$ a.u. for the short-range and polarization terms. For the present case of low-energy electron-helium scattering we use the polarizability of helium $\alpha_p=1.383\,19$ a.u. and let Z be an adjustable parameter to give the best possible representation of the measured field-free scattering. This procedure leads to $Z=1.07$ for the best fit. In Table I we show the absolute values of the differential cross section at 2 eV as measured by Andrick and Bitsch [10], their statistical errors, and our calculated value from the above potential. We see that our values for most angles are within a few percent of their measured values and well within their statistical errors.

TABLE I. Comparison of measured [10] e-He elastic scattering differential cross section at 2 eV with the present theoretical model.

θ (deg)	Measured $d\sigma_{\rm el}/d\Omega$ (statistical error) (in 10^{-6} cm^2/sr)	Present model $d\sigma_{\rm el}/d\Omega$
15	0.230 (0.029)	0.244
20	0.255 (0.023)	0.258
25	0.272 (0.021)	0.274
30	0.282 (0.019)	0.290
35	0.290 (0.018)	0.306
40	0.299 (0.017)	0.322
45	0.322 (0.016)	0.339
50	0.335 (0.015)	0.357
55	0.357 (0.014)	0.375
60	0.377 (0.014)	0.395
65	0.394 (0.013)	0.415
70	0.410 (0.013)	0.434
75	0.437 (0.012)	0.454
80	0.470 (0.012)	0.473
85	0.489 (0.011)	0.493
90	0.511 (0.011)	0.513
95	0.534 (0.011)	0.532
100	0.541 (0.011)	0.552
105	0.557 (0.015)	0.570
110	0.591 (0.015)	0.588
115	0.601 (0.015)	0.605
120	0.616 (0.015)	0.621
125	0.618 (0.015)	0.637
130	0.648 (0.015)	0.651
135	0.647 (0.016)	0.665
140	0.672 (0.015)	0.678
145	0.687 (0.016)	0.688

This gives us confidence that the present perturbative results will also be quantitatively accurate.

This $V(r)$, as a static potential, has one bound s state. This is not inconsistent with the fact that there are no bound states of the real He^- system. The absence of a physical bound state is a result of the fact that a full three-electron antisymmetric trial wave function would not give an expectation value of the total energy that lies below the ground-state energy of He. Thus, approximating e-He scattering by the static potential $V(r)$ amounts to using a model that gives a good representation of the low-energy electron scattering phase shifts while not being a good indicator of the bound-state structure of the composite system. At the relatively low laser intensities presently considered the bound electrons will only be slightly perturbed by the laser field [12], and the predominant interaction effects are expected to be between the laser field and the scattering electron, as assumed in our present perturbative analysis.

IV. RESULTS AND DISCUSSION

The numerical solution of the radial Schrödinger equation allows the evaluation of all $v_l(r)$ and $\eta_l(k)$ (radial wave functions and phase shifts, described in [8]) and the first- and

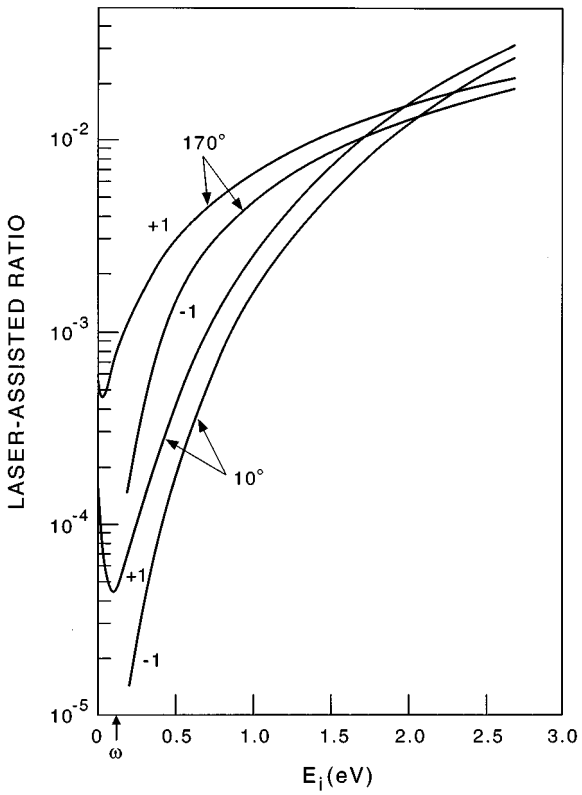

FIG. 1. Calculated laser-assisted ratios for one-photon absorption (+) and emission (−) for scattering angles 10° and 170°, intensity 1×10^6 W/cm^2, and polarization along direction of incidence.

second-order radial matrix elements

$$R(lk,l'k')=\int_0^\infty dr\; v_l \frac{dV}{dr} v_{l'},$$

$$\mathcal{R}(l_ik_i\rightarrow l\rightarrow l_fk_f)=\int_0^\infty dk\; \frac{R(l_ik_i,lk)R(lk,l_fk_f)}{(k^2\pm k_0^2)}, \quad (6)$$

which are needed for the cross sections in Eq. (4) using the partial-wave expansions given in the Appendix of [8]. All measurements of these processes are in the form of the ratio of scattered electron counts in a particular time interval during the laser pulse to elastically scattered electron counts in an equal field-free time interval. The identical values of scattering angle θ and acceptance element of solid angle $d\Omega$ ensure that this ratio is equivalent to $(d\sigma^{(n)}/d\Omega)/(d\sigma_{\rm el}d\Omega)$. The conservation of electron number (not flux) further leads to the sum rule

$$\frac{d\sigma_{\rm el}}{d\Omega}=\sum_{n=-\infty}^{\infty}\frac{k_i}{k_f}\frac{d\sigma^{(n)}}{d\Omega}. \quad (7)$$

This means that the occurrence of inelastic free-free processes in the laser pulse must be accompanied by a reduction in the elastic scattering cross section, i.e., $d\sigma^{(0)}/d\Omega < d\sigma_{\rm el}/d\Omega$. In Figs. 1 and 2 we give the variation with electron energy for one- and two-photon processes at $\theta=10°$ and 170°. The angular variation of these cross sections

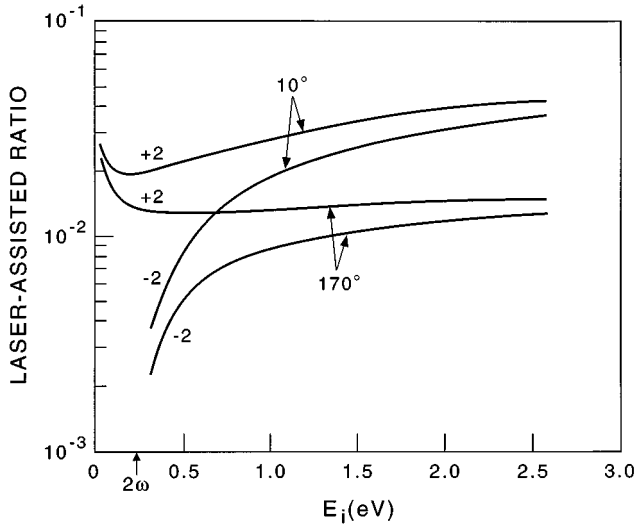

FIG. 2. Same as for Fig. 1, but for the two-photon case.

between these limits is smooth and without any special structures. The fact that the laser-assisted ratio for absorption is larger than that for emission is consistent with preliminary measurements at these energies [9].

We have also looked at the predictions of the Kroll-Watson formula over the range of parameters covered in Figs. 1 and 2 and find that they give laser-assisted ratios that in most cases lie many orders of magnitude below those given by perturbation theory. The only exception is for large-angle scattering with one-photon transfer, where the Kroll-Watson was within a factor 2 of the perturbation theory results, an agreement that must be regarded as fortuitous. We thus confirm our findings in [8] that the Kroll-Watson formula is very unreliable at low electron energies.

We would also like to point out another limit in which the Kroll-Watson formula

$$\frac{d\sigma^{(n)}}{d\Omega}=\frac{k_f}{k_i}J_n^2\left(\frac{\mathbf{E}_0}{\omega^2}\cdot(\mathbf{k}_i-\mathbf{k}_f)\right)\frac{d\sigma_{\rm el}}{d\Omega} \quad (8)$$

appears to fail. For laser polarizations perpendicular to the scattering plane the argument of the Bessel function will vanish identically, which would predict that there is zero probability for n-photon transfer for any $n\neq0$ and that the elastic scattering would be unchanged for the laser on or laser off. This is in contrast to the perturbation theory result for that laser polarization, which is vanishing probability only for odd n. To date all experiments have been done with polarization in the scattering plane, perhaps because of the expectation from the Kroll-Watson formula. It would be interesting to see if the perpendicular polarization would result in the elimination of only the odd n peaks, as is expected from perturbation theory.

The curves for emission have thresholds at $E_i=n\omega$. In Fig. 3 we give the one-and two-photon results as a function of E_i at $\theta=160°$ on a linear scale. This allows us to get a better overall picture of the approaches to thresholds. The threshold energy dependences may be understood by looking at the limiting forms the matrix elements in Eq. (4). By referring to Eq. (A1) in [8] we see the limiting behavior at zero energy,

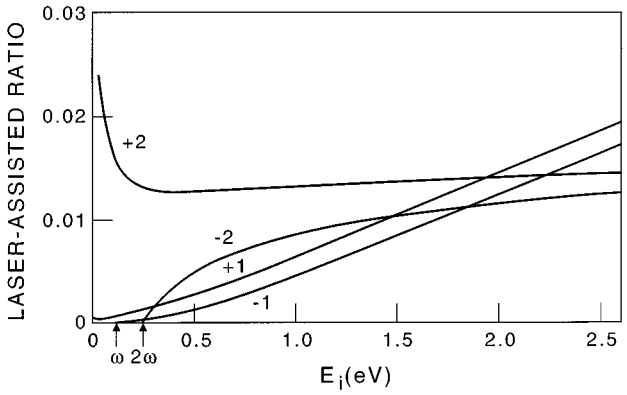

FIG. 3. Calculated laser-assisted ratios for one- and two-photon processes at scattering angle 160°, intensity 1×10^6 W/cm^2, and polarization along the direction of incidence.

$$M^{(++)}_{\mathbf{k}_f\mathbf{k}_i} \xrightarrow[k_i\to 0]{} \frac{\text{const}}{k_i}\times R(1k_f,0k_i)\propto \text{const}, \tag{9}$$

since $R(1k_f,0k_i)\propto k_i$ in that limit. The same limiting behavior in $M^{(++)}_{\mathbf{k}\mathbf{k}_i}$ will also make the effective matrix element for n-photon absorption approach a constant as k_i or $E_i\to 0$. This leads to all n-photon absorption cross sections behaving as k_i^{-1} in the zero-energy limit. In Fig. 3 this limiting form is much more apparent in the $n=+2$ result than for $n=+1$. The thresholds for n-photon stimulated emission occur at $E_i=n\omega$ and will be governed by

$$M^{(++)}_{\mathbf{k}_f\mathbf{k}} \xrightarrow[k_f\to 0]{} \frac{\text{const}}{k_f}\times R(0k_f,1k)\propto \text{const}. \tag{10}$$

This leads to the threshold forms k_f^2 or $E_i-n\omega$, i.e., linear in the excess energy. Again in Fig. 3, this is much more apparent in the $n=-2$ result than for $n=-1$.

It is somewhat surprising that the two-photon cross sections are larger than the one-photon ones at low energies. This is different from the relative values we found at 10 eV in [8], where the one-photon cross sections are above the two-photon ones, but we have checked that such a reversal does indeed result from the numerics of the phase shifts and radial matrix elements. In Fig. 4 we show the perturbation theory results for one- and two-photon absorption at $E_i=1$ eV and $\theta=160°$ as a function of laser intensity. The present perturbative results, which we believe to be valid for $I\leqslant 10^6$ W/cm^2, are shown as the solid lines of slopes 1 and 2 on the log-log plot. From their linear extensions it is seen that they would intersect the upper bound of 1 at higher intensities. This means that the exact nonperturbative results must bend over. We do not know the exact form since we have no available reliable theory there. Preliminary data of Wallbank [9] suggest that at $I=5\times10^7$ W/cm^2 the values are as indicated by the points in Fig. 4. Those measurements were taken for the slightly different conditions of $\theta=156°$ and laser polarization along the momentum transfer direction. Possible smooth joinings of the lowest-order perturbation theory to these points are indicated. These would represent the departure of the correct result from lowest-order perturbation theory at higher intensities. We hope that additional measurements at lower intensities will allow a direct comparison with the perturbative results.

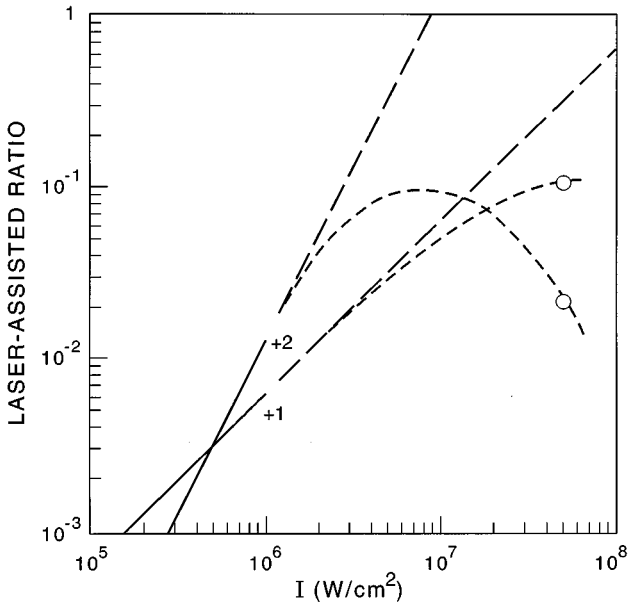

FIG. 4. Intensity variation of laser-assisted ratios for one- and two-photon absorption at $E_i=1$ eV. The solid straight lines for $I<1\times10^6$ W/cm^2 are obtained from perturbation theory for $\theta=160°$ and polarization along the direction of incidence. Their linear extensions to higher intensities are indicated with long dashes. Preliminary measurements [9] at $I\cong5\times10^7$ W/cm^2 are given by the points. A possible set of joinings between the data points and the perturbative calculations are indicated by the short-dashed lines.

V. ELASTIC SCATTERING IN THE LASER PULSE

As discussed in [8] the requirement of particle conservation must apply to the scattered electrons, and this is equivalent to the conservation of probability of n-photon transfer, or

$$\sum_{n=-\infty}^{\infty} P_n = 1, \tag{11}$$

where these transfer probabilities are related to their respective cross sections by

$$\frac{d\sigma^{(n)}}{d\Omega} = \frac{k_f}{k_i} P_n \frac{d\sigma_{\text{el}}}{d\Omega}. \tag{12}$$

The laser-assisted ratios of cross sections $(d\sigma^{(n)}/\,d\Omega)/(d\sigma_{\text{el}}/d\Omega)$ are plotted in Figs. 2–4, so the P_n's are given by k_i/k_f times these ratios. Since $k_f=k_i$ for $n=0$, the ratio of elastic scattering for laser on to laser off is P_0, and by the conservation law (11) this is

$$P_0 = 1-\sum_{n\neq 0} P_n. \tag{13}$$

A consequence of this is that the elastic-scattering cross section with the laser on $d\sigma^{(0)}/d\Omega$ (or its ratio to $d\sigma_{\rm el}/d\Omega$) will have discontinuities in slope as E_i crosses new inelastic thresholds at $n\omega$ (n-photon emissions). This is expected because the perturbative result for n-photon absorptions, which depends on η_l and R, will have continuous behavior through the various emission thresholds. Since we presently evaluate P_n for only $n=\pm 1$ and ± 2 we are unable to use Eq. (13) to make an accurate evaluation of P_0. We could do this if all contributions for $|n|\geqslant 3$ turned out to be negligible at this intensity, but we have no reason to expect that to be so, especially since $P_2 > P_1$ here.

A direct evaluation of P_0 from $\psi^{(2)}$ would involve the interference between the second-order terms in $e^{i\omega_{kk_i}t'}$ in Eq. (3) and the field-free amplitude, but does not appear to be feasible because of the lack of exact unitarity in the truncated perturbative wave function. Another way of understanding this is that there are contributions from all P_n for $n\neq 0$ to P_0 in the conservation law (13), so one could not expect that $\psi^{(2)}$ alone would be adequate for its direct evaluation.

Note added in proof

The work referred to in [9] has recently been published (to be referred to as WH) [B. Wallbank and J. K. Holmes, J. Phys. B **29**, 5881 (1996)]. We make the following observations:

(1) The ratios for measured one-photon absorption to emission in the laser-assisted signals given in WH, Fig. 3 (at $I\cong 5.8\times 10^7$ W/cm^2, $\theta=156°$), are very close to those in our Fig. 1 (at $I=10^6$ W/cm^2, $\theta=170°$).

(2) The points in their Fig. 3 that WH attribute to our calculation are probably in error due to a misunderstanding in our communication. Our perturbation theory calculation was carried out at the lower intensity of 10^6 W/cm^2. The theory and experiment can only be compared by an extrapolation such as given in our Fig. 4. The value of the measured laser-assisted ratio given in that figure is a factor of 3 higher than that given in WH, Fig. 3, to approximately account for the fact that their electron beam is about three times wider than their laser beam (private communication from WH).

(3) In the data shown in WH, Fig. 2, it is seen that the sum rule given in Eq. (13) is roughly satisfied. The laser-assisted signal given in WH, Fig. 2, for 0 photons is equivalent to our P_0-1.

ACKNOWLEDGMENT

I am indebted to Barry Wallbank for helpful discussions and communications.

[1] A. Weingartshofer, J. K. Holmes, G. Caudle, E. M. Clarke, and H. Krüger, Phys. Rev. Lett. **39**, 269 (1977).

[2] A. Weingartshofer, E. M. Clarke, J. K. Holmes, and C. Jung, Phys. Rev. A **19**, 2371 (1979).

[3] A. Weingartshofer, J. K. Holmes, J. Sabbagh, and S. L. Chin, J. Phys. B **16**, 1805 (1983).

[4] N. M. Kroll and K. M. Watson, Phys. Rev. A **8**, 804 (1973).

[5] B. Wallbank and J. K. Holmes, Phys. Rev. A **48**, R2515 (1993).

[6] B. Wallbank and J. K. Holmes, J. Phys. B **27**, 1221 (1994).

[7] B. Wallbank and J. K. Holmes, J. Phys. B **27**, 5405 (1994).

[8] S. Geltman, Phys. Rev. A **53**, 3473 (1996). We make note here of two corrections for this reference: (i) the expressions for the n-photon effective cross sections in Eq. (9) should have an additional factor k_f/k_i, which is very close to 1 for the $E_i=10$ eV of that paper, and appears in the present Eq. (4); and (ii) a computer programming error was made that caused the one-photon perturbation theory results given in that paper to be a factor 16 too low (see Figs. 2, 4, 6, and 8 therein). This does not affect any of our conclusions, as the comparisons with experiment were made for relative cross sections.

[9] B. Wallbank (private communication).

[10] D. Andrick and A. Bitsch, J. Phys. B **8**, 393 (1975).

[11] F. V. Bunkin and M. V. Fedorov, Zh. Eksp. Teor. Fiz. **49**, 1215 (1965) [Sov. Phys. JETP **22**, 844 (1966)].

[12] S. Geltman, Phys. Rev. A **51**, R34 (1995).